Supplementary Materials I

Our experimental strategy, the magnetic tweezers, entails the anchoring of a single linear double-stranded (ds)DNA molecule between a coated glass surface and a coated paramagnetic bead[1], and is schematically depicted in SM Figure 1. An upward magnetic stretching force F on the DNA is generated by means of a pair of magnets positioned above the sample. By changing the distance from the magnets to the sample, F can be varied, and by rotating the magnets about their axis, supercoils can be mechanically injected. By continuously monitoring the height of the bead above the surface, *i.e.* the DNA extension, the degree of supercoiling σ can be determined in real time.

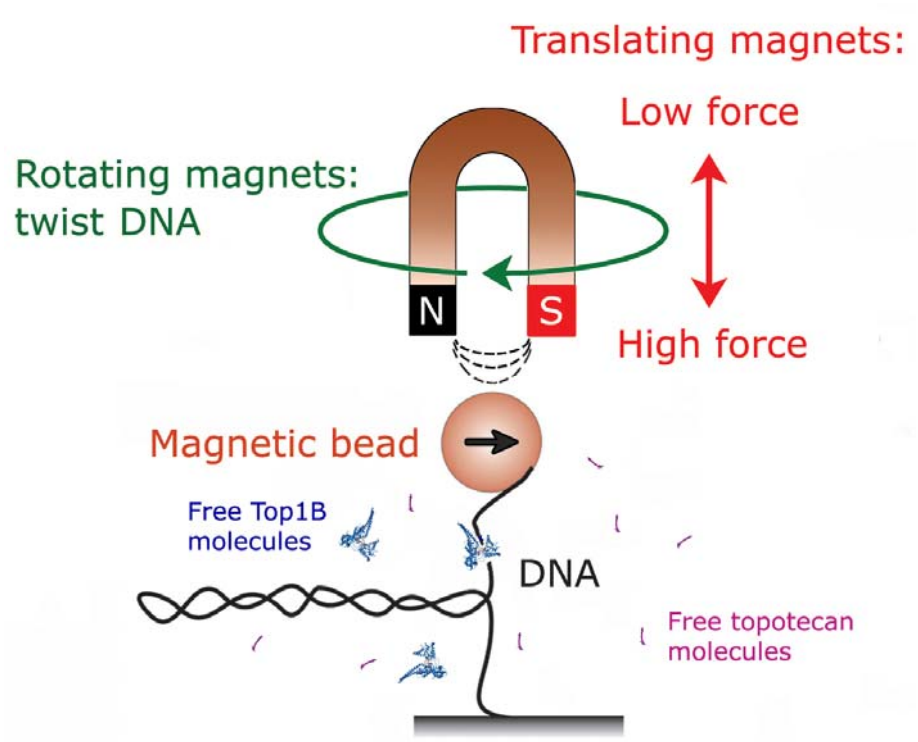

SM Figure 1. Schematic representation of the magnetic tweezers setup. A pair of magnets mounted above the flowcell exerts an upward stretching force on a magnetic bead, which in our configuration has a diameter of 1 μm. A (ds)DNA molecule that contains multiple biotin groups at one end is bound to a streptavidin-coated bead. Multiple digoxigenin groups are attached to the other end of the DNA molecule, resulting in the tethering of the DNA molecule to the anti-dogoxigenin-coated surface. The multiple linkages ensure that the ends of the DNA molecule are rotationally constrained. As such, rotating the magnets twists the (ds)DNA molecule, leading to the introduction of plectonemic supercoils that are subsequently removed by Top1B molecules (not drawn to scale) present in the solution surrounding the DNA/bead construct. Free topotecan molecules are also present in the solution.

Supplementary Materials II

As has been shown for vaccinia virus Top1B[2], human Top1B does not always relax all DNA plectonemes present in the DNA in a single enzymatic event (Fig. 1a of main text). S.M. Figure 2 contains a collection of traces that exhibit this distributive behaviour of human Top1B.

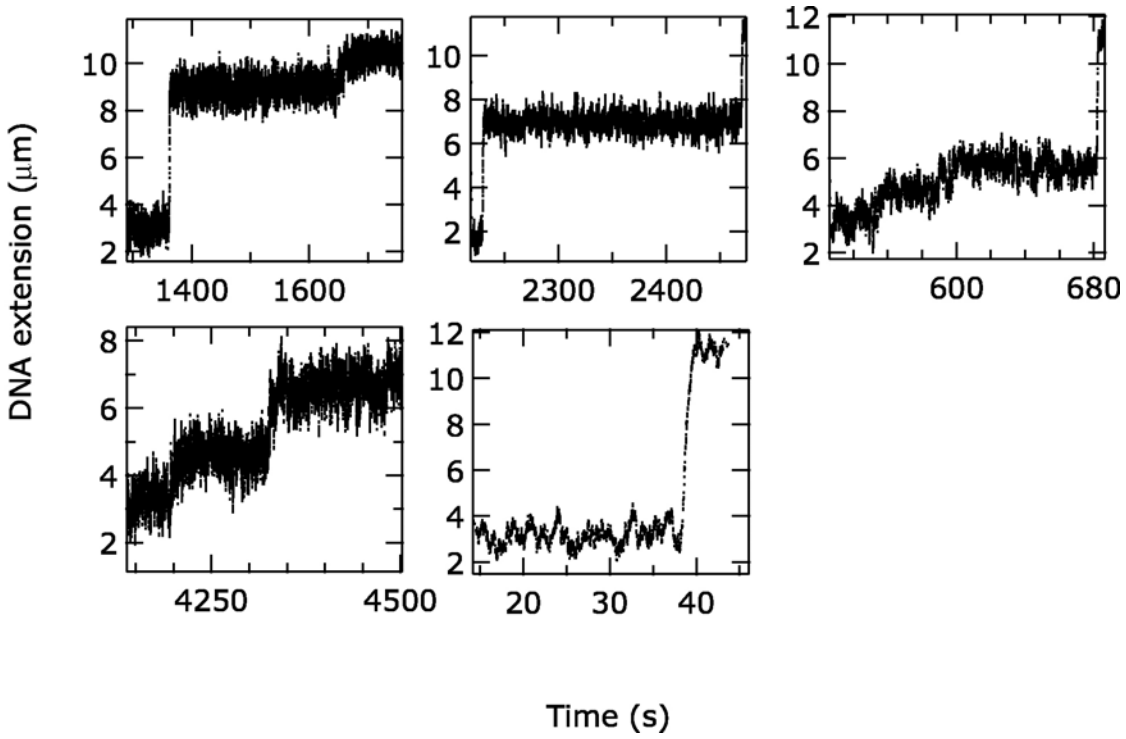

SM Figure 2. A collection of traces demonstrating that human Top1B can exhibit step-wise supercoil relaxation. The duration of the plateaus separating cleavage-religation cycles is dependent on the concentration of Top1B.

Supplementary Materials III

We show that the DNA extension velocity during topotecan-mediated Top1B uncoiling is independent of the ratio between the Top1B concentration and the topotecan concentration, as shown in SM Figure 3.1, where the ratio is varied by a factor of 25. The change in ratio is primarily achieved by changing the topotecan concentration, as the Top1B concentration is only varied by a factor of 2. Decreasing the Top1B concentration further decreases the frequency of uncoiling event below reasonable experimental timescales. Increasing the Top1B concentration may cause artifacts of Top1B clustering that we avoid[3]. We note that the uncoiling velocities shown in SM Figure 3.1 are not measured in a topotecan concentration-saturated regime, as a further slight decrease of the topotecan concentration leads to the disappearance of slow uncoiling within reasonable experimental timescales. The uncoiling events that are observed at such lower topotecan concentrations are fast and indistinguishable from Top1B-mediated uncoiling events in the absence of topotecan. These arguments suggest that a single topotecan molecule is responsible for the slow uncoiling that is observed.

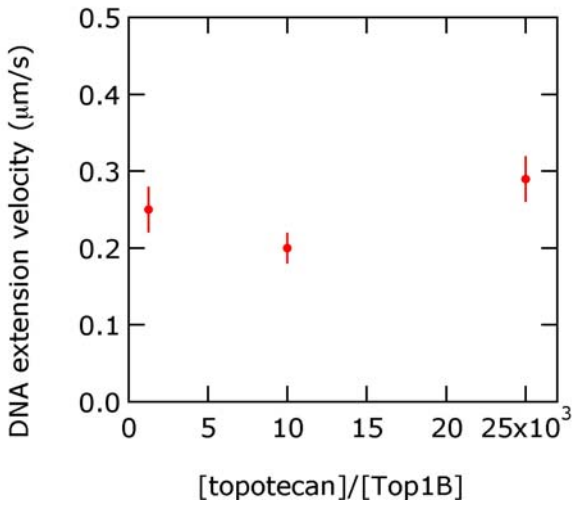

SM Figure 3.1. The DNA extension velocity of topotecan-mediated uncoiling is independent of the ratio of topotecan concentration, [TPT], to Top1B concentration, [Top1B].

Furthermore, we show that the time during which slow uncoiling is observed, $\langle \Delta t \rangle$ (see main text), is independent of the topotecan concentration. This is important in light of a potential concern that $\langle \Delta t \rangle$ might be an overestimate if multiple topoisomerase enzymes, each associated with topotecan, induce successive slow uncoiling events separated by intervals smaller than our time resolution. If this were the case, however, one would expect $\langle \Delta t \rangle$ to depend on the topotecan concentration, with low topotecan concentrations

leading to shorter <Δt> and high topotecan concentrations leading to longer <Δt>. However, over the range of topotecan concentrations tested (which range from a lower limit below which no further slow relaxation events are observed to an upper concentration approaching the limit of topotecan solubility), no observable change in <Δt> is observed in our data (SM Figure 3.2). Thus, our measurement of <Δt> is not likely to be overestimated by multiple topotecan-bound Top1B molecules acting in parallel.

Indeed, our measurement of Δt may instead represent a lower limit for the time topotecan remains bound, since t_{end} can be caused by topotecan exiting from the covalent complex as described in the main text, or, in principle, by the start of topotecan-independent uncoiling by a second Top1B at another cleavage site on the DNA. To exclude this possibility within the narrow range of practical Top1B concentrations, we have verified that the measurement of <Δt> was unaltered upon changing the Top1B concentration by a factor of 2.

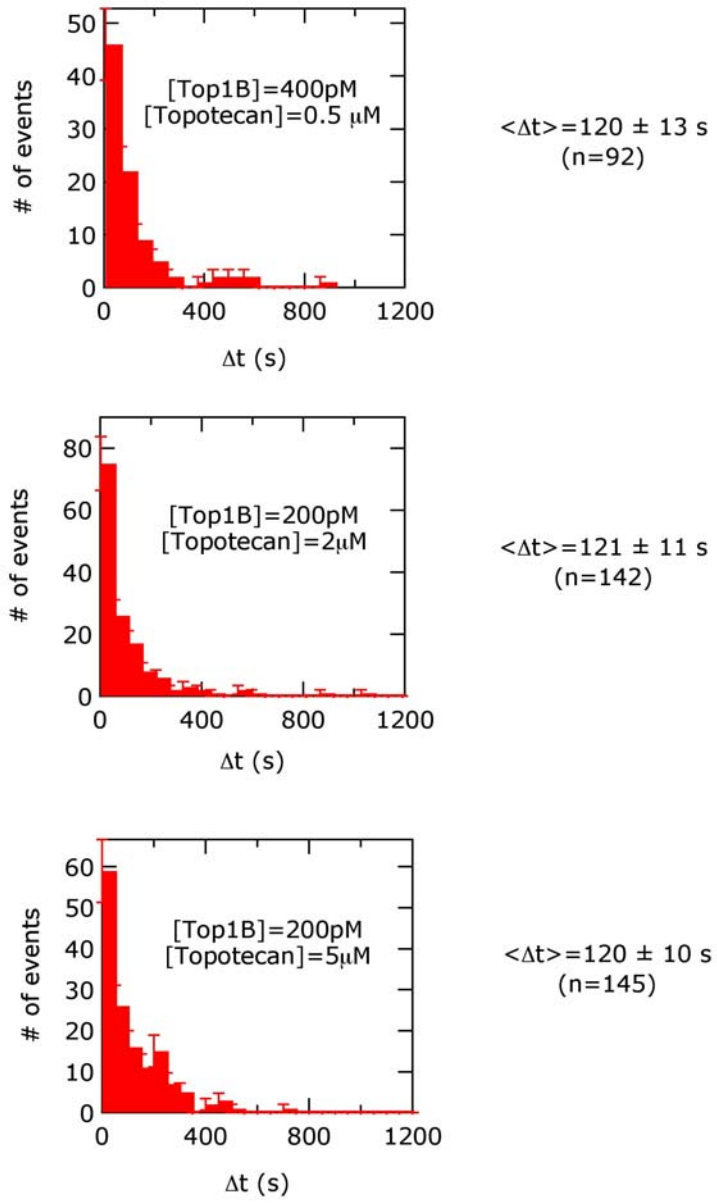

SM Figure 3.2. Upon varying the topotecan concentration by an order of magnitude, we do not observe a change in <Δt>. This leads us to conclude that the measurement of <Δt> is not influenced by the topotecan concentration.

Supplementary Materials IV

We show that topotecan-mediated supercoil removal occurs at thermodynamic equilibrium, allowing us to faithfully convert (linear) DNA extension velocities to angular velocities of DNA rotation. SM Figure 4 shows the strategy for demonstrating this. First we measure the DNA extension as a function of magnet rotation, where each measurement point constitutes an average over 5 seconds and the waiting time between measurements is >10 s (SM Figure 4a). The values for the DNA extension obtained in this manner can be assumed to equal the equilibrium values. From these measurements, we extract the linear slope by fitting to a linear relation (red line), corresponding to the gain (or loss) in DNA extension upon removal (or addition) of plectonemes in the constant torque (writhe) regime, e.g. 36 nm/turn at a stretching force of 0.9 pN. We then measure the DNA extension as a function of time, while continuously rotating the magnets at a preset and known angular velocity (SM Figure 4b). We again fit the linear part of the increase in DNA extension with a linear relation and obtain a number for the DNA extension velocity at this given magnet rotation rate. We verify that the DNA molecule completes as many rotations as the magnets. From these two measurements, we can calculate the inferred angular velocity of the DNA. This procedure is repeated for various preset magnet rotation speeds and the inferred DNA rotation rate is plotted against the preset magnet rotation speed, as shown in SM Figure 4c. It is clearly seen that the two quantities are in excellent agreement with each other and that a faithful measurement of the DNA rotation rate can be made by measuring the DNA extension velocity, at least up to 3 Hz.

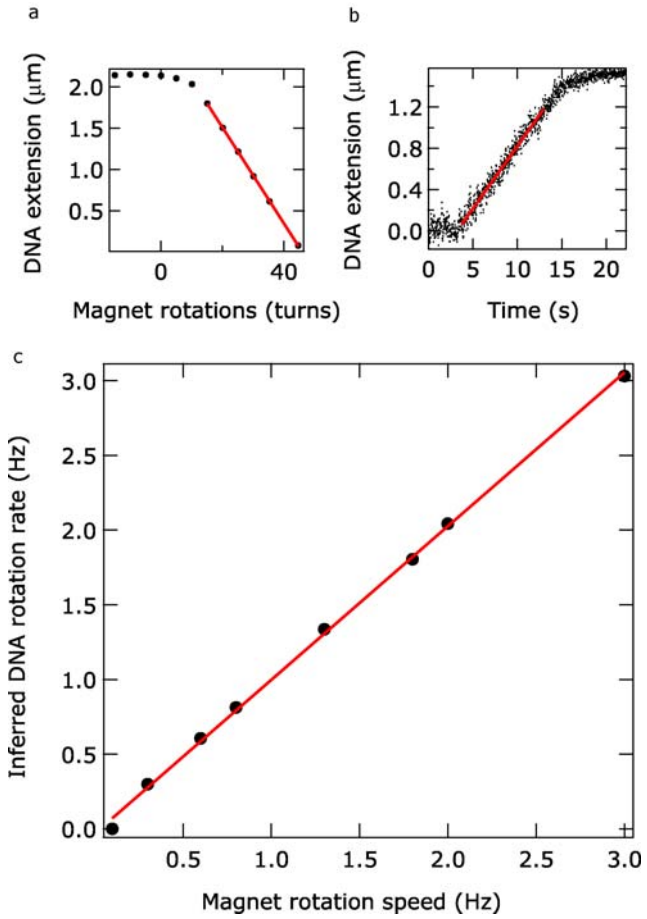

SM Figure 4. The strategy for proving that topotecan-mediated slow DNA uncoiling proceeds at thermodynamic equilibrium. **a**, the equilibrium measurement of the DNA extension vs. the number of magnet rotations. In the Writhe regime, where all additional twisting of the DNA molecule leads to the formation of plectonemic supercoils, we fit a linear relation (red line). **b**, the DNA extension as a function of the time during which the DNA molecule is uncoiled at a constant angular velocity. The resulting increase in DNA extension is also fitted with a linear relation (red line). **c**, the angular velocity of the magnets (magnet rotation speed) *vs.* the angular velocity of the DNA rotation (inferred DNA rotation rate), as calculated using the values obtained from the linear fits **a** and **b** (see the Supplementary Materials IV text for a detailed description of the calculation). The regime of angular velocities probed here includes the angular velocity of topotecan-mediated uncoiling of DNA, as described in the main text.

Supplementary Materials V

We show that the global mechanical properties of bare DNA are unaltered upon addition of 5 μM of topotecan in the same buffer used in the other experiments (SM Figure 5.1). The slow enzymatic uncoiling observed in the presence of topotecan can thus not be explained by a global stiffening or by a global change in the torque response of DNA.

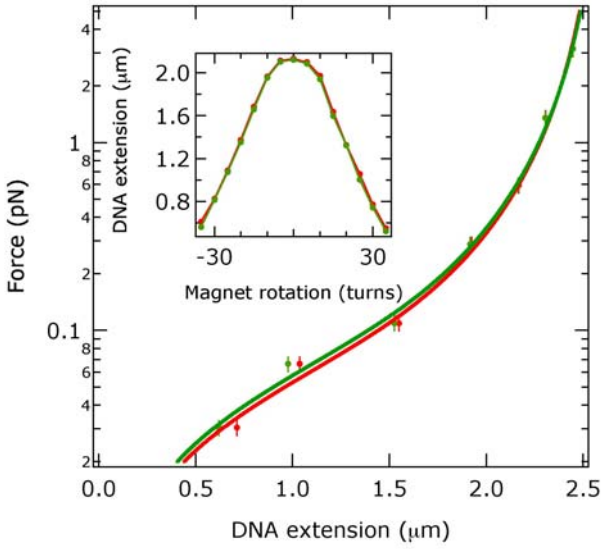

SM Figure 5.1 Force-extension and supercoiling (inset) behaviour of bare double-stranded DNA in the presence (red) and absence (green) of 5 μM of topotecan.

Several control experiments were also performed to exclude the possibility that non-specific Top1B-topotecan interactions could give rise to the slow uncoiling described above. First, we incubated human Top1B in the presence of camptothecin, the parent compound of topotecan that induces a similar mechanism of Top1B poisoning[4]. SM Figure 5.2a shows a similar signature as that seen with topotecan, indicating that the effects observed were not uniquely limited to the water-soluble topotecan analog. Second, we studied uncoiling by vaccinia virus topoisomerase I, known to be resistant to camptothecins[5], in the presence of high concentrations of topotecan. Here, we reproduced the characteristic step-wise uncoiling (SM Figure 5.2b) that was observed before in the absence of topotecan[2] and that does not feature continuous slow uncoiling at concentrations similar to and higher than those used in the experiments with human Top1B. Third, we generated a single nick in the DNA by incubating the DNA with the sequence-specific nicking enzyme N.BbvCIA. By subsequently rotating our magnets, we attempted to introduce plectonemes in the presence of topotecan alone (SM Figure 5.2c),

and in the presence of topotecan and the catalytically inactive human Top1Y723F (SM Figure 5.2d). In both experiments, no plectonemes could be introduced, in contrast to the results obtained in the presence of catalytically active human Top1B and topotecan (Figure 1b in the main text). These experiments show that a catalytically active human Top1B is required to yield slow uncoiling, consistent with the *in vivo* activity and co-crystal structures of camptothecin analogues[6-8]. We thus conclude that slow uncoiling represents a clear signature for a topotecan molecule bound to the Top1B-DNA complex.

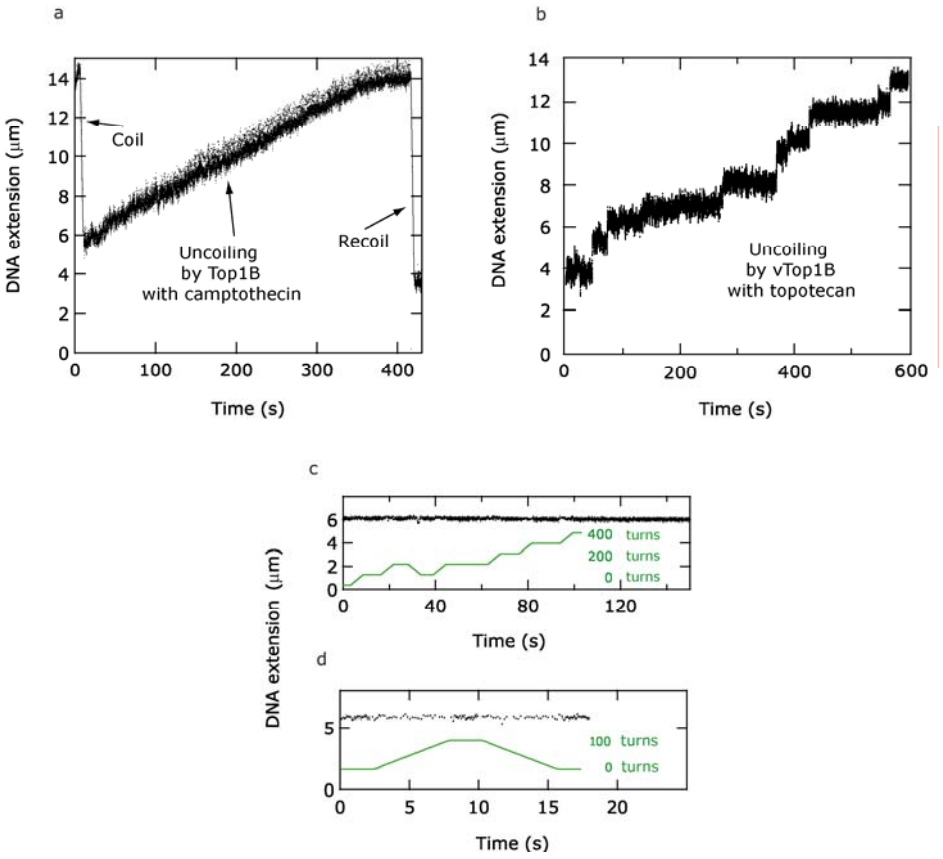

SM Figure 5.2. Control experiments that show that a catalytically active human Top1B is required for the observation of slow uncoiling in the presence of camptothecin or topotecan. **a**, Human Top1B in the presence of camptothecin yields slow uncoiling very similar to that observed with the clinical analogue topotecan. **b**, In the presence of topotecan, slow continuous supercoil removal is not observed with the camptothecin-resistant vaccinia Top1B. **c**, Neither positive supercoils nor plectonemes can be induced by mechanical coiling of a singly nicked DNA molecule in the presence of topotecan only, or **d**, in the presence of topotecan and catalytically inactive human Top1Y723F.

Supplementary Materials VI

Here we describe the strategy for measuring the religation time, *i.e.* the time interval between cleavage of the DNA by Top1B and subsequent religation. The time that Top1B remains covalently trapped on the DNA in the presence of topotecan (as described in the main text) ought to be compared with this time in the absence of the drug. SM Figure 6.1 depicts the strategy for measuring this quantity. When Top1B nicks the DNA (at t_{nick}) and the bead consequently travels upwards due to DNA uncoiling, it reaches above a threshold (at t_{rotate}), beyond which we prompt the magnets to spin continuously. In the absence of topotecan, DNA uncoils faster than the magnets can recoil. Consequently, plectonemes are removed and the bead keeps traveling upwards until Top1B religates the DNA and plectonemes can be once again introduced (at $t_{religated}$). The religation time is then calculated according to $t_{religation} = t_{religated} - t_{nick}$.

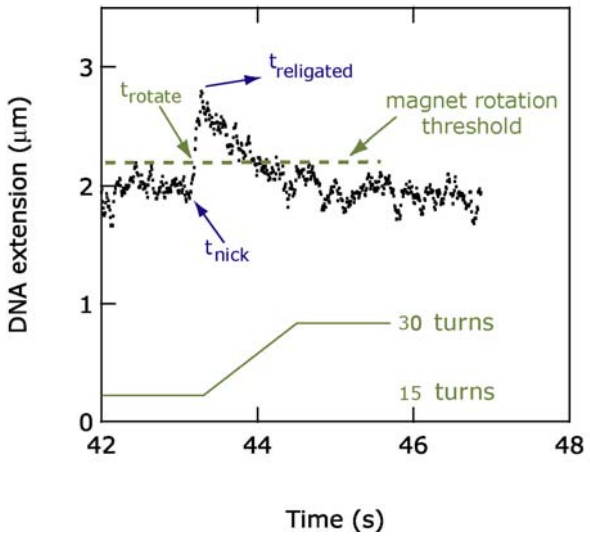

SM Figure 6.1. Strategy for measuring Top1B religation time in the absence of topotecan, as described in the text of supplementary materials VI.

As described in supplementary materials II, not all injected plectonemes are always removed in a single enzymatic event. Here we present a technical point concerning the implications of the latter for the measurement of the religation time.

If, following a single enzymatic event, plectonemes remain in the DNA, the religation time is measured as described above. Above a threshold in DNA extension (set above the experimental noise of the bead), which is crossed soon after Top1B nicks the DNA (at t_{nick}), the magnets spin continuously (red blocks in SM Figures 6.2a-c). At a certain point in time, the DNA is religated by Top1B and continuous rotation of the magnets will then lead to mechanical addition of plectonemes and consequently to a decrease in DNA

extension. This point in time, designated $t_{religated}$, is used to calculate the religation time according to $t_{religation} = t_{religated} - t_{nick}$, as described above.

However, a subtle complication occurs when all plectonemes are removed from the DNA in a single enzymatic event. In this case, the magnets continue to impose rotation on the bead after all plectonemes have been removed, *i.e.* the DNA is rotated while at $\sigma=0$, and the DNA extension initially remains constant, as shown in SM Figure 6.2b. At a later point in time during the continuous coiling of the DNA, the Top1B religates the DNA, and plectonemes can once again be introduced ($t_{religated}$ in SM Figure 6.2b). However, monitoring of the supercoiling state in the magnetic tweezers is largely limited to the observation of the plectonemic regime, which occurs beyond the buckling instability[9]. The time ΔT_{delay} it takes to reach this buckling instability from $\sigma=0$ therefore needs to be substracted from the religation time. Thus for events in which all plectonemes are removed in a single enzymatic events, the correct religation time is $t_{religation} = t_{religated} - t_{nick} - \Delta T_{delay}$. SM Figure 6.2c shows the procedure for measuring ΔT_{delay}. Starting at $\sigma=0$ (at 59 s) we continuously rotate the magnets at the maximum angular velocity that the stepper motor, which rotates the magnets, allows. For our experimental configuration, this is 30 Hz. We monitor the DNA extension and observe at what time plectonemes appear. ΔT_{delay}, is calculated by substracting the time at $\sigma=0$ from the time at which plectonemes form, as shown in SM Figure 6.2c. The correct value of $t_{religation}$ is computed taking ΔT_{delay} into account.

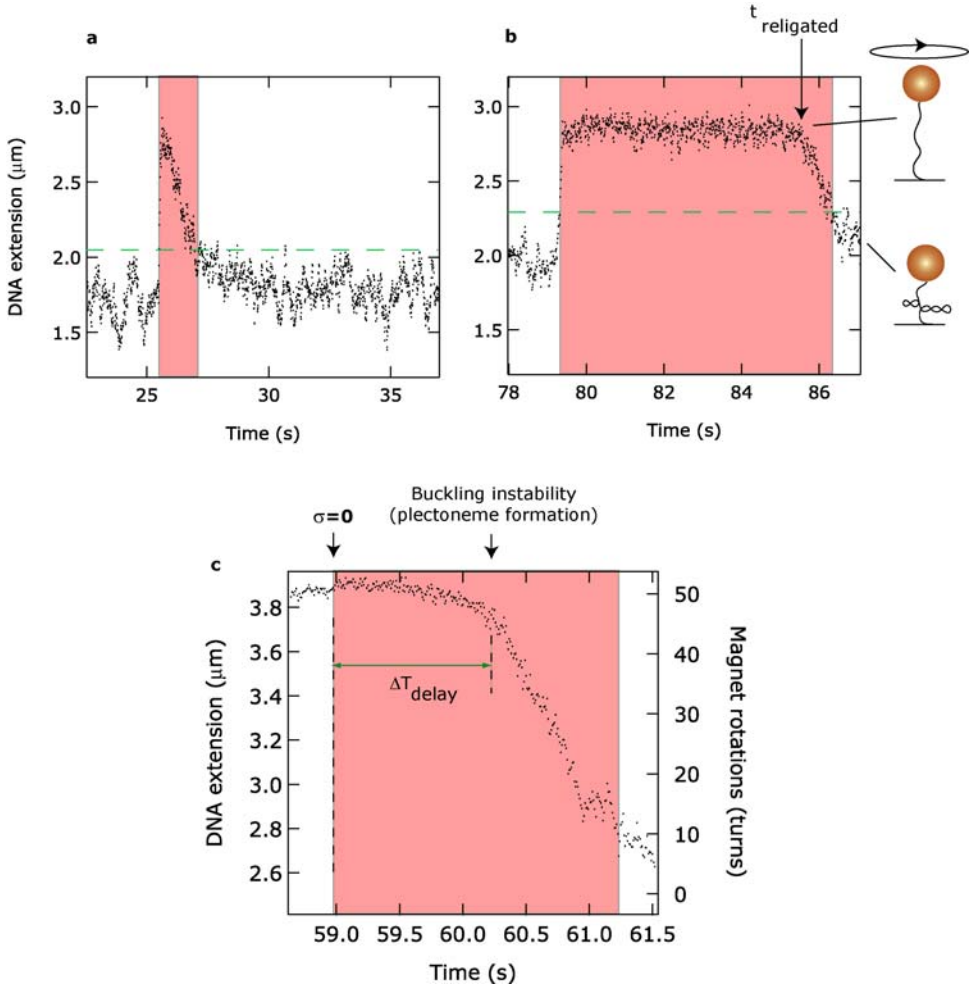

SM Figure 6.2. Strategy for measuring the religation time of Top1B. **a**, When plectonemes remain in the DNA following a single enzymatic event, religation effectively results in an immediate decrease of the DNA extension. The religation time, $t_{religation}$, is then readily obtained by calculating $t_{religation} = t_{religated} - t_{nick}$, as described in the main text. **b**, However, when all plectonemes are removed from the DNA in a single enzymatic event, a systematic correction of the religation time needs to be taken into account. The correction is the time delay between the instant of religation and the instant at which plectonemic supercoils form. **c**, This time delay, ΔT_{delay}, is measured by continuously twisting a DNA molecule from $\sigma=0$ (at 59.0 s) to the onset of the formation of plectonemes (the buckling instability, at 60.2 s) and is approximately 1.2 s. The correct calculation for the religation time incorporates the correction according to $t_{religation} = t_{religated} - t_{nick} - \Delta T_{delay}$.

Supplementary Materials VII

Here we present velocities for uncoiling of positive (+) versus negative (-) supercoils in the absence of topotecan. As can be seen from the distributions shown in SM Figure 7**a** (removal of positive supercoils) and **b** (removal of negative supercoils), any difference between the distributions is fairly minor given the broadness of the velocity distributions (mean values of 4.5 ± 1.4 and 3.3 ± 2, respectively).

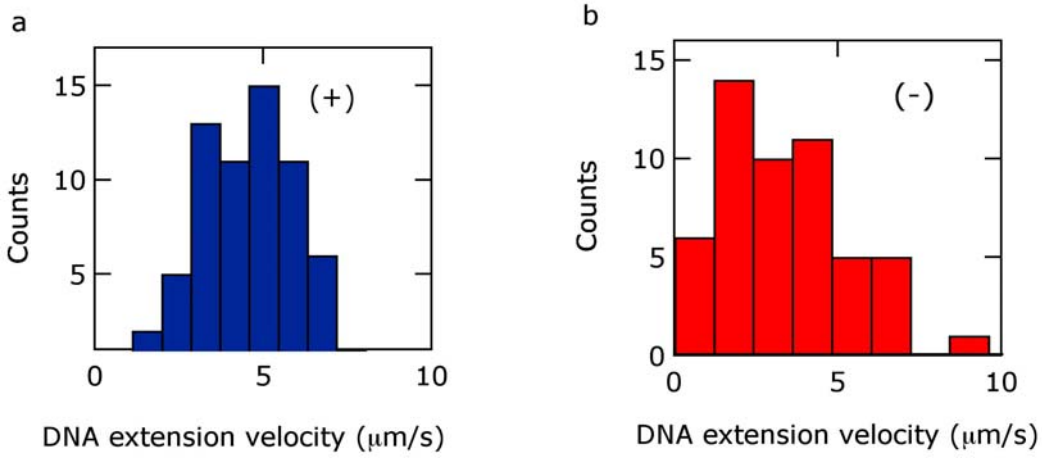

SM Figure 7. DNA extension velocities during uncoiling of positive (a) and negative (b) supercoils.

Furthermore, we find that in the absence of camptothecin, expression of Top1B in yeast cells does not skew the topoisomer distribution *in vivo* (Fig. 4c and d of main text), consistent with our single-molecule experiments indicating no significant difference in the rate of enzyme-catalyzed uncoiling of positive *vs.* negative supercoils.

A number of other studies have addressed the binding to and relaxation of positive versus negative supercoils. Molecular dynamic simulations describe distinct mechanisms for positive and negative supercoil relaxation in the absence of topotecan[10], but cannot address the relative relaxation rates. Recent biochemical studies suggest higher levels of Top1B-DNA complexes are formed with positively *vs.* negatively supercoiled DNA and that this bias is increased in the presence of camptothecin[11]. However, our *in vivo* results show that this increased level of complexes does not correlate with preferential cleavage of positively supercoiled DNA by Top1B, since such preferential cleavage (and relaxation) might be expected to skew the distribution towards more negative supercoils, in contrast to what is observed in our data (Fig. 4c and d of main text).

Supplementary Materials VIII

In this part of the Supplementary Materials, we explain the principle of two-dimensional gel electrophoresis.

For a double-stranded plasmid DNA of a given size, the overall compaction of the molecule will determine its electrophoretic mobility in an agarose gel[12]. The topological state of a plasmid is described by the linking number (Lk), which is the sum of two geometrical properties, the twist (Tw) plus the writhe (Wr). Tw describes the number of times one strand wraps around the other and Wr describes the coiling of the helical axis of the DNA. Plasmid DNAs of identical sequence, but with different Lk, can be resolved in agarose gels on the basis of their Wr, where the Wr of a DNA topoisomer being considered is proportional to ΔLk, the difference between the Lk of the plasmid topoisomer being considered and what the Lk of the same plasmid would be if it were relaxed. Under physiological conditions, the latter may be approximated by (size of plasmid in bp) / (10.5 bp per helical turn). The Lk of an intact circular plasmid is invariant and will always be an integral value. However, the relative contribution of Tw and Wr may vary.

As an example, let us consider a negatively supercoiled 2,100 bp plasmid DNA with an Lk of 192. The same plasmid, when relaxed, would have an Lk of 200. We also assume that the entire Lk deficit is partitioned into Wr, such that Lk = Tw + Wr is described by 192 = 200 + (-8), as shown for form I in SM Figure 8a. If this plasmid is incubated with increasing concentrations of the DNA intercalator chloroquine (indicated by grey rectangles) and in the absence of a topoisomerase, the decrease in Tw induced by chloroquine binding will induce a compensatory increase in Wr, since Lk must remain constant. As depicted in SM Figure 8a, the effect of increasing chloroquine binding (decreased Tw and increased Wr) will affect the compaction of the molecule and hence its electrophoretical mobility. In the absence of chloroquine, the DNA would be very compact (Wr = -8, SM Figure 8a. I) and migrate rapidly; in a gel containing low concentrations of chloroquine (such that Wr = -4, SM Figure 8a. II), it would migrate more slowly, and at somewhat higher concentrations of chloroquine (such that Wr = 0, SM Figure 8a. III), it would migrate more slowly still. However, at even higher concentrations of chloroquine, the DNA would acquire a positive Wr (Wr = +4, SM Figure 8a. IV), and would again migrate more rapidly, as if positively supercoiled.

These same principles apply to the electrophoretic resolution of plasmid DNA topoisomers in two dimensions. In the first dimension (indicated by the vertical arrow in SM Figure 8b), the DNAs are resolved in the presence of low concentrations of chloroquine, such that a DNA topoisomer with a slight deficit in Lk would acquire the lowest Wr and run at apex I (SM Figure 8b). DNAs of lower or higher Lk would migrate with a mobility difference proportional to absolute value of the linking number difference from the topoisomer at apex I. The gel is then rotated 90˚ and run in a second dimension (indicated by the horizontal arrow in SM Figure 8b) in the presence of an increased concentration of chloroquine. Here, a plasmid of even lower Lk will now acquire the lowest Wr (apex II, S.M. Figure 8b). As in the first dimension, DNAs of lower or higher

Lk will now migrate with a mobility difference proportional to the absolute value of the linking number difference from the topoisomer at apex II. Once the gel has been run in the two dimensions with the different chloroquine concentrations as described, a topoisomer arc as diagrammed in SM Figure 8b results, where a given topoisomer spot differs from the adjacent spot by a linking number difference of one. This analysis permits a clear discrimination between plasmids with a linking number deficit, which are skewed towards the lefthand side of the arc, and plasmids with a linking number excess, which are skewed towards the righthand side of the arc. Plasmid DNA that is nicked is free to assume the most relaxed conformation and will migrate at the apex in both dimensions, as shown.

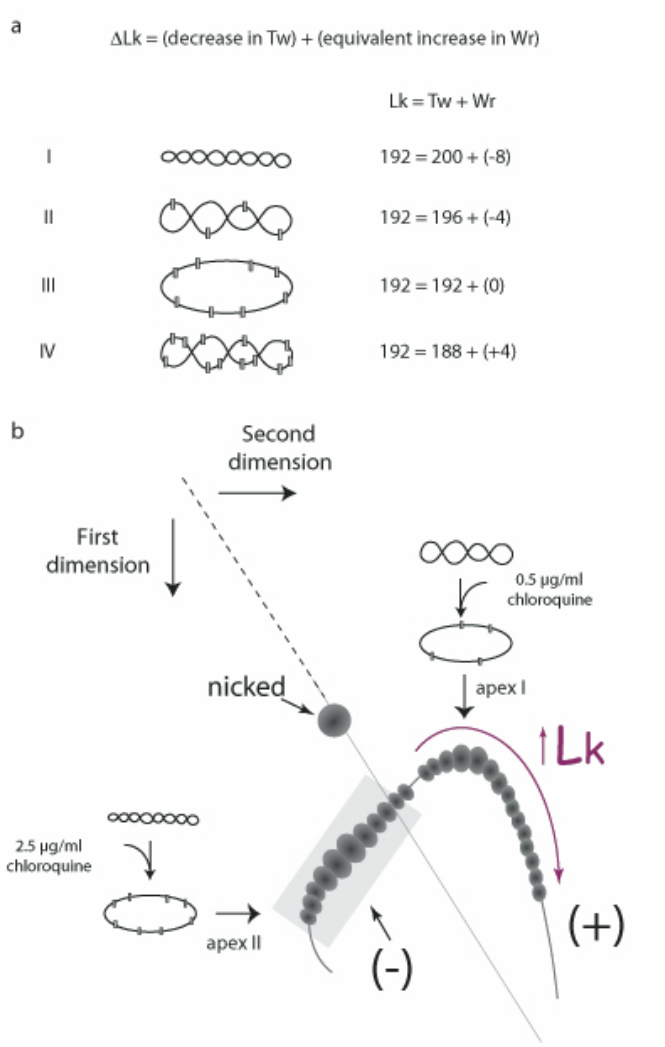

SM Figure 8. Topological isomers of DNA can be resolved using 2D agarose gel electrophoresis.

Supplementary Materials IX

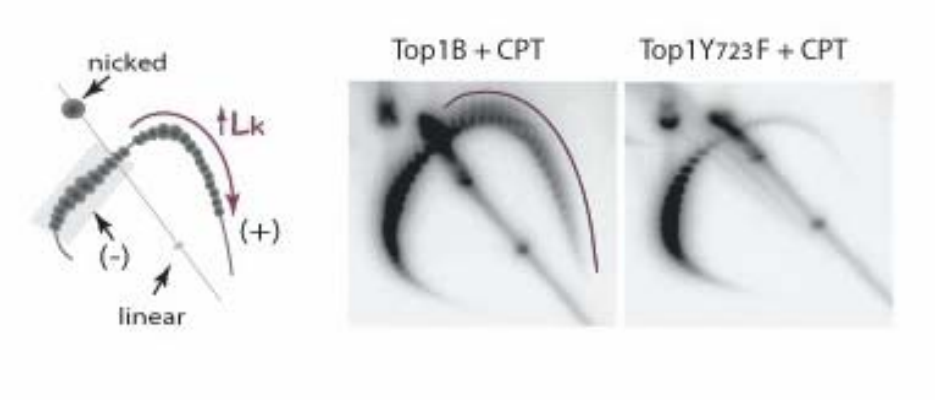

SM Figure 9. Camptothecin-induced accumulation of positive supercoils requires the expression of catalytically active Top1B. Exponential cultures of *top1Δ*, *top2ts* cells [yeast strain JCW28 (MAT**a**, *top1*Δ*, top2*^{ts})[13]], transformed with plasmids expressing low levels of wild-type human Top1B or the catalytically inactive human Top1Y723F mutant, were shifted to 36˚C for 1 hour to inactivate Top2, then treated with camptothecin (CPT) for 30 minutes. The resulting distribution of 2 μm plasmid DNA topoisomers was assessed in 2-D gels, as described in the main text. These data demonstrate expression of a catalytically active Top1B is necessary for camptothecin-induced accumulation of positive supercoils (purple arc).

Supplementary Materials X

The main text describes the accumulation of positive supercoils in both G1-phase and S-phase cells that include normal levels of wild-type yeast Top2. Here we show the analysis of 2 μm plasmid topoisomers after camptothecin treatment of *top1Δ* cells expressing a thermosensitive mutant of Top2, denoted *top2*^{ts}. When these cells are shifted to the non-permissive temperature (36˚C), Top2 activity is largely abolished. In these experiments, α -factor arrested cells were shifted to 36˚C for two hours with additional α-factor, then treated as described in the text. For G1-phase arrested cells and in the absence of drug (upper row in SM Figure 10a), one observes an expected bias in the plasmid topoisomer distribution towards negative supercoils, as explained in the main text. However, camptothecin treatment of Top1B-expressing cells induces skewing of the plasmid topoisomer distribution (purple arcs), which persists throughout G1 phase. By contrast, no alteration in linking number was induced by camptothecin treatment of cells that expressed only a vector control and were lacking Top1B. A similar picture emerges from the topoisomer distribution analysis of cells that were allowed to transit S-phase synchronously (SM Figure 10b). Also here, only the combined treatment of drug and expression of Top1B gave rise to the accumulation of positive supercoils. In wild-type *TOP2* cells, ~20% of plasmid DNA topoisomers exhibiting an increase in linking number as a consequence of Top1B poisoning by camptothecin in G1 or S-phase (described in main text). However, in the absence of Top2, the proportion of plasmid DNA topoisomers with increased linking number was increased to >30% in G1-phase and to values exceeding 50% as cells transit S-phase. These data indicate that Top2 activity is insufficient to resolve all the positive supercoils that accumulate as a consequence of the asymmetric DNA uncoiling induced by camptothecin poisoning of Top1B, but does play a role.

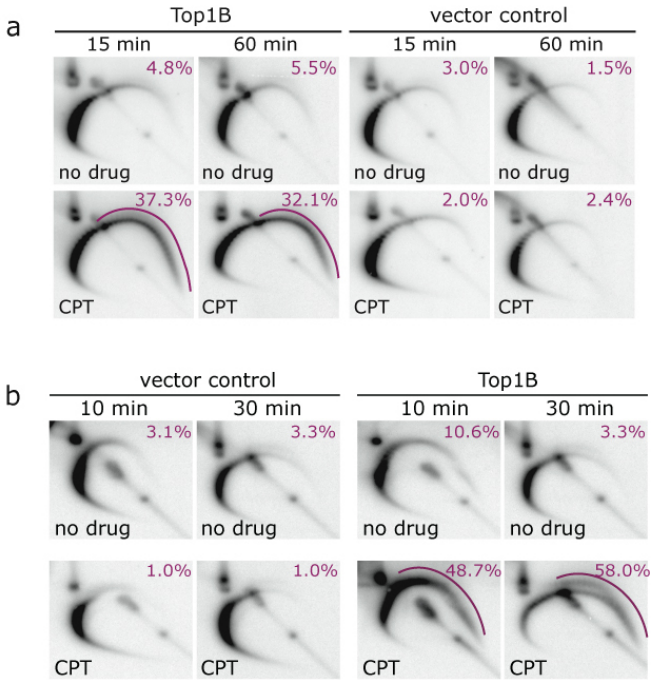

SM Figure 10. Positive supercoils accumulate in both G1-phase (**a**) and S-phase (**b**) after camptothecin treatment of *top1Δ, top2*^{ts} cells that were shifted to the non-permissive temperature, at which Top2 activity is largely abolished. Purple numbers indicate the percentage of topoisomers exhibiting an increase in linking number, as determined by PhosphorImage analysis.

Supplementary Materials XI

We show that camptothecin treatment of yeast cells, as they synchronously transit S-phase of the cell cycle, induces Top1B-dependent DNA damage which has modest effects on cell viability, yet nonetheless suffices to trigger the slow kinetics of S-phase transit characteristic of S-phase checkpoint activation. Yeast *top1Δ* cells, transformed with a plasmid that expresses low levels of human Top1B or an empty vector control were arrested in G1-phase with the mating phermone α-factor and then released into S-phase in the presence or absence of camptothecin (CPT).

In panel **a**, samples of cells, taken at the times indicated, were serially ten-fold diluted and 5 µl aliquots were spotted onto agar plates. Following incubation at 30˚C, cell viability was assessed by the formation of colonies. The viability of untreated Top1B expressing cells (labelled Top1B), or untreated or camptothecin vector control cells (labelled vector control and vector control + CPT, respectively) was unchanged during the course of the experiment. Top1B expressing cells treated with camptothecin (labelled Top1B + CPT) began to exhibit a slight reduction in cell viability at 40 minutes following release into S-phase, with about a 10-fold reduction in cell viability relative to 0 time evident at 60 minutes drug treatment.

As shown in panel **b**, the cell cycle distribution of cells, treated as in panel a, was also assessed. Cells taken at the indicated times were fixed with 70% ethanol, stained with propidium iodide and assayed for DNA content by flow cytometry[14]. The peak height reflects the number of cells in the sample, while the distribution along the X axis is an indication of DNA content. Haploid yeast cells in G1 phase of the cell cycle accumulate with a 1N DNA content, while cells in G2/M phases of the cell cycle have a 2N DNA content. As cells transit S-phase, DNA content increases from 1N to 2N. In untreated Top1B expressing cells and in the untreated or CPT treated vector controls, the cells exhibit a similar pattern of S-phase progression, with the majority of cells in G2/M phase at 60 minutes as indicated by the presence of a 2N peak. In contrast, camptothecin treatment of Top1B expressing cells (Top1B + CPT) exhibit a slow, synchronous transit through S-phase which results from DNA damage-induced activation of the S-phase checkpoint.

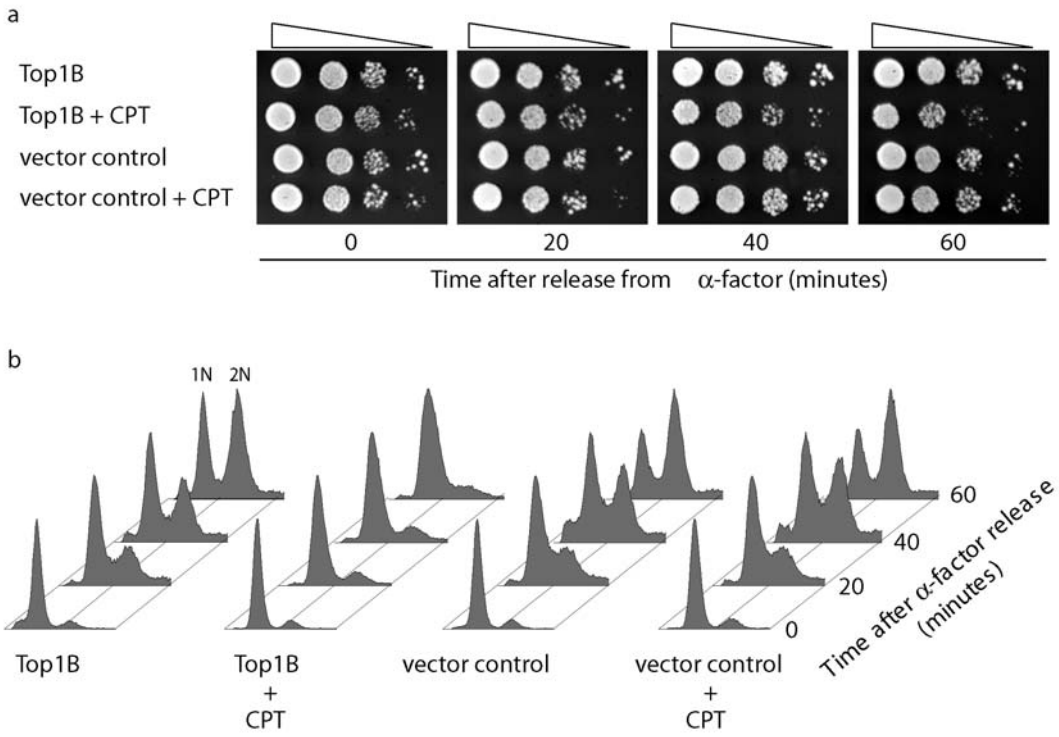

SM Figure 11. Camptothecin treatment of yeast cells in S-phase induces a Top1B-dependent decrease in cell viability (**a**) and a delay in cell cycle progression (**b**).

References

1. Smith, S. B., Finzi, L. & Bustamante, C. Direct mechanical measurements of the elasticity of single DNA molecules by using magnetic beads. Science 258, 1122-6 (1992).
2. Koster, D. A., Croquette, V., Dekker, C., Shuman, S. & Dekker, N. H. Friction and torque govern the relaxation of DNA supercoils by eukaryotic topoisomerase IB. Nature 434, 671-4 (2005).
3. Moreno-Herrero, F. et al. Atomic force microscopy shows that vaccinia topoisomerase IB generates filaments on DNA in a cooperative fashion. Nucleic Acids Res 33, 5945-53 (2005).
4. Slichenmyer, W. J., Rowinsky, E. K., Donehower, R. C. & Kaufmann, S. H. The current status of camptothecin analogues as antitumor agents. J Natl Cancer Inst 85, 271-91 (1993).
5. Shuman, S., Golder, M. & Moss, B. Characterization of vaccinia virus DNA topoisomerase I expressed in Escherichia coli. J Biol Chem 263, 16401-7 (1988).
6. Chrencik, J. E. et al. Mechanisms of camptothecin resistance by human topoisomerase I mutations. J Mol Biol 339, 773-84 (2004).
7. Staker, B. L. et al. The mechanism of topoisomerase I poisoning by a camptothecin analog. Proc Natl Acad Sci U S A 99, 15387-92 (2002).
8. Woo, M. H., Vance, J. R., Marcos, A. R., Bailly, C. & Bjornsti, M. A. Active site mutations in DNA topoisomerase I distinguish the cytotoxic activities of camptothecin and the indolocarbazole, rebeccamycin. J Biol Chem 277, 3813-22 (2002).
9. Strick, T., Allemand, J., Croquette, V. & Bensimon, D. Twisting and stretching single DNA molecules. Prog Biophys Mol Biol 74, 115-40 (2000).
10. Sari, L. & Andricioaei, I. Rotation of DNA around intact strand in human topoisomerase I implies distinct mechanisms for positive and negative supercoil relaxation. Nucleic Acids Res 33, 6621-34 (2005).
11. McClendon, A. K., Rodriguez, A. C. & Osheroff, N. Human topoisomerase IIalpha rapidly relaxes positively supercoiled DNA: implications for enzyme action ahead of replication forks. J Biol Chem 280, 39337-45 (2005).
12. Hanai, R. & Roca, J. DNA topoisomerase protocols: DNA topology and enzymes. (eds. Bjornsti, M.-A. & Osheroff, N.) (Humana Press, NJ, 1999).
13. Hann, C. et al. Increased camptothecin toxicity induced in mammalian cells expressing Saccharomyces cerevisiae DNA topoisomerase I. J Biol Chem 273, 8425-33 (1998).
14. Haase, S. B. & Lew, D. J. Flow cytometric analysis of DNA content in budding yeast. Methods Enzymol 283, 322-32 (1997).